

Bypass Heat Sink Analysis for a Laser Diode Bar with a Top Canopy

Byeong-Gwan Ji, Seung-Gol Lee, Se-Geun Park, and Beom-Hoan O*

Department of Information and Communication Engineering, INHA University, 100 Inha-ro,
Nam-gu, Incheon 402-751, Korea

(Received August 30, 2016 : revised January 25, 2017 : accepted April 5, 2017)

With the increasing use of high-power laser diode bars (LDBs) and stacked LDBs, the issue of thermal control has become critical, as temperature is related to device efficiency and lifetime, as well as to beam quality. To improve the thermal resistance of an LDB set, we propose and analyze a bypass heat sink with a top canopy structure for an LDB set, instead of adopting a thick submount. The thermal bypassing in the top-canopy structure is efficient, as it avoids the cross-sectional thermal saturation that may exist in a thick submount. The efficient thickness range of the submount in a typical LDB set is guided by the thermal resistance as a function of thickness, and the simulated bypassing efficiency of a canopy is higher than a simple analytical prediction, especially for thinner canopies.

Keywords : Diode laser arrays, Laser diode bars, Pumping Laser diode, DPAL

OCIS codes : (230.0230) Optical device; (140.2010) Diode laser arrays; (140,3480) Lasers, diode-pumped; (140.3580) Lasers, solid-state

I. INTRODUCTION

The laser diode bar (LDB) has found increasing numbers of applications, such as in pumping lasers and direct tools for material processing, by virtue of its higher Electro-Optic conversion efficiency, compact size, and long lifetime [1, 2]. As the need for producing high optical power increases, issues of cooling and packaging become important for stable high-power operation [3-5]. Designing an efficient heat sink for an LDB requires various considerations, such as the removal of thermal bottlenecks to obtain a low thermal resistance, matching thermal expansion coefficients for a long lifetime [6], and maintaining compact size. It is then important to consider the design limitations of the submount thickness for an LDB set for high-power applications, particularly for stacked LDBs. A heat-sink design with a top-canopy structure for improved thermal resistance is reported here, and the efficiency of relieving the thermal bottleneck and the limiting conditions of thickness control are discussed for a typical LDB, by comparing the predicted results to those simulated using ANSYS Icepak, a commercial 3D computational fluid dynamics (CFD) tool.

II. THERMAL ANALYSIS OF LDB STRUCTURE

A typical structure of stacked LDBs of *p*-side down LD with an additional water-cooling system on the back side is shown in Fig. 1.

The height of each LDB set h_{total} is the thickness of an LDB with submount heat-sink structure. Assuming that the

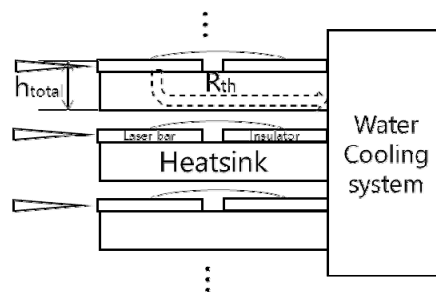


FIG. 1. Conceptual side view of typical stacked LDBs and an additional backside water-cooling system (right in the figure). The thermal flow is denoted by dashed arrows. R_{th} is the corresponding effective thermal resistance.

*Corresponding author: obh@inha.ac.kr

Color versions of one or more of the figures in this paper are available online.



This is an Open Access article distributed under the terms of the Creative Commons Attribution Non-Commercial License (<http://creativecommons.org/licenses/by-nc/4.0/>) which permits unrestricted non-commercial use, distribution, and reproduction in any medium, provided the original work is properly cited.

heat transferred to the backside water-cooling system is removed efficiently, the submount heat-sink design needs to lower as much as possible the thermal resistance R_{th} of the submount under each LDB. Although it is apparent that a higher h_{total} results in lower R_{th} , h_{total} must be minimized to raise the LDB stacking density for high power applications. An analysis of R_{th} for a typical LDB set is compared to that for a proposed LDB assembly with a top canopy, as shown in Fig. 2.

The circuit diagram of a simplified thermal-resistance-network model with R_H (submount heat sink), R_{LD} (LD substrate), and R_C (top canopy) is also included. Note that typical LDB sets use a thick Cu/W submount heat sink and bonding wires, without the top-canopy structure. Although the thermal conductivity of Cu is higher than that of Cu/W, Cu/W is a common contact material for an LDB, due to its mechanical strength and coefficient of thermal expansion (CTE). As the CTE of a thin (7 μm) solder layer is almost double that of GaAs, it requires a Cu/W submount and buffer layers on top. An LDB integrates many laser-emitter stripes into a linear array on a chip. An LDB is typically 10 mm wide, 0.1 mm high, and the cavity length of each emitter stripe is between 0.6 and 2.0 mm. Considering the typical width of 150-200 μm for the emitter stripe and a pitch (repetition length of emitter stripes) of 400-500 μm , the filling factor ranges from 30 to 50% [6]. The heat generated in the active layers of each LDB is transferred to the backside heat sink chiefly by thermal conduction, at a rate of more than $\sim 99\%$ in most cases, according to preliminary simulations. Because the contributions of air conduction and surface radiation at the laser bar become more negligible as the stacking density increases, the thermal analysis hereafter considers solely thermal conduction.

The heat flow from the active region to the backside

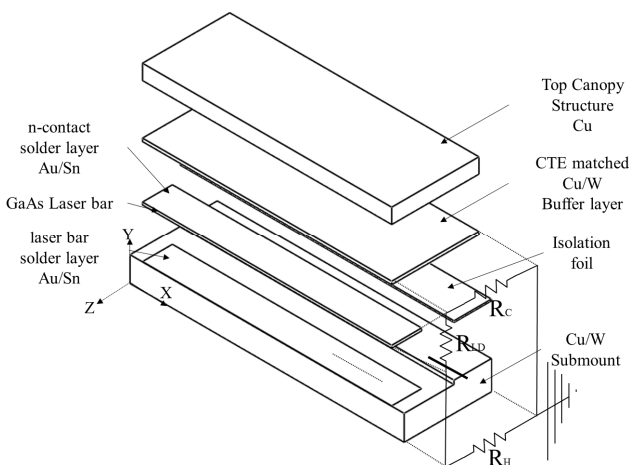


FIG. 2. Assembly drawing of a proposed LDB set (LDB on a heat-sink submount) with a top canopy. The thermal-resistance circuit diagram of a simplified network model is drawn on the right side.

heat sink through the Cu/W submount is shown in Fig. 3. The simulation conditions are set at 50 W for the heat power and 25°C for the backside interface temperature.

The lines of equal temperature are drawn in Fig. 3(a). The left figure is for the case of a bottom heat-sink thickness $h = 800 \mu\text{m}$, while that on the right is for $h = 1800 \mu\text{m}$. As the heat diverges from the center of the active region of an LDB, the heat streamline resembles a quasihyperbolic curve, similar to the thermal divergence model [8]. The curve of R_{th} as a function of h , shown in Fig. 3(b), is just the connected guideline of simulated values of R_{th} (CFD simulated result, CsR) at several h values, denoted by closed circles. The dotted line is an inverse- h ($\sim 1/h$) curve fit of simulated R_{th} values for $h < 800 \mu\text{m}$. The extended $\sim 1/h$ curve (dotted line) deviates from the guideline at $h > 800 \mu\text{m}$, which means that thermal divergence is more significant for large h , and the thermal flow is deformed from simple laminar flow, and thus the effective cross-sectional area is reduced as h increases. It is interesting that the problem of thermal-flow deformation is not severe for $h < 800 \mu\text{m}$, where one would intuitively expect the thermal bottleneck to be

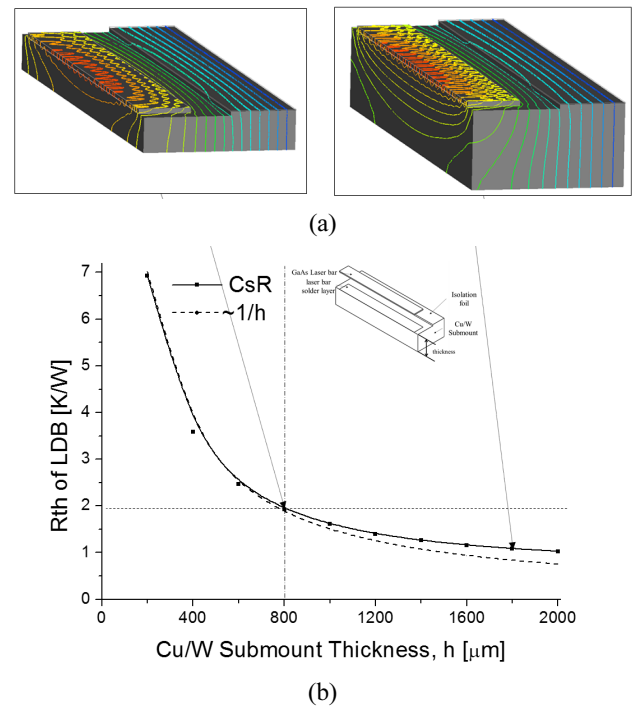


FIG. 3. Thermal-resistance variation of a conventional LDB without a top canopy is simulated as a function of submount thickness: (a) Contour map of lines of equal temperature for two cases of thickness $h = 800$ and $1800 \mu\text{m}$. Note that the vertical equi-temperature lines under the LDB are more tilted for a thicker submount; (b) Thermal-resistance values from CsR for various submount thicknesses are denoted as closed circles, and the line is a guide to the eye. The dashed line is the simply-approximated thermal-resistance result, with a functional dependence of $\sim 1/h$.

TABLE 1. Values of the geometrical parameters path length, height, and width, and of the thermal conductivity, used in the simulation. [7, 8]

Part	Dimensions (μm) X \times Y \times Z	Thermal Conductivity K(W/mK)
Cu/W submount	11000 \times 800 \times 3500 & 11000 \times 94 \times 1500	200 (Cu/W)
Laser bar Solder Layer	10000 \times 7 \times 1200	48 (AuSn)
Laser bar based GaAs	10000 \times 100 \times 1200	44 (GaAs)
n-contact Solder Layer	10000 \times 7 \times 1200	48 (AuSn)
CTE matched Cu/W Buffer Layer	10000 \times 100 \times 3500	200 (Cu/W)
Top Canopy Cu Structure	10000 \times 400 \times 3500	400 (Cu/W)
Isolation foil	11000 \times 20 \times 1500	4

significant. The value of the simulated thermal resistance R_{th} between any two points of interest on the same heat streamline is obtained from Eq. 1,

$$R_{th} = \Delta T / P \quad (1)$$

where ΔT is the temperature difference between the two points and P is the heat power transmitted along the path. For straight, laminar thermal flow, it is simple to formulate R_{th} using geometrical parameters, such as the path length and cross-sectional area, plus the thermal conductivity, as denoted in Eq. 2,

$$R_{th} = l / k(h \cdot w) \quad (2)$$

where l is the thermal path length, k is the thermal conductivity of the material, h is the thickness, w is the width, and $h \times w$ is the cross-sectional area of the thermal path. This simple model explains the reason for the good curve fit of R_{th} for $h < 800 \mu\text{m}$. The geometrical parameters, such as the path length, height, and width, and the

materials with their thermal conductivities used in the simulation are listed in Table 1 [7, 8].

As seen in Fig. 3(b), simply increasing h is not efficient for lowering R_{th} , and the thermal divergence problem gets more severe for $h > 800 \mu\text{m}$. Here a heat sink with a top-canopy structure (TCS) is proposed to improve R_{th} without the drawbacks of the thermal divergence problem.

III. THERMAL ANALYSIS OF THE PROPOSED LDBs

The TCS with contact electrodes provides a thermal bypass. The TCS is a copper plate attached on top of a Cu/W buffer layer with matching coefficient of thermal expansion (CTE). The simulated results are shown in Fig. 4. Figure 4(a) shows the temperature distribution with lines of equal temperature for a top-canopy thickness $h_c = 400 \mu\text{m}$ and $h = 800 \mu\text{m}$, which results in $R_{th} = 0.94 \text{ K/W}$. The CsR values of R_{th} for various h_c (fixed $h = 800 \mu\text{m}$, solid line) and h (fixed $h + h_c = 1200 \mu\text{m}$, dotted line), and the corresponding guidelines, are shown in Fig. 4(b).

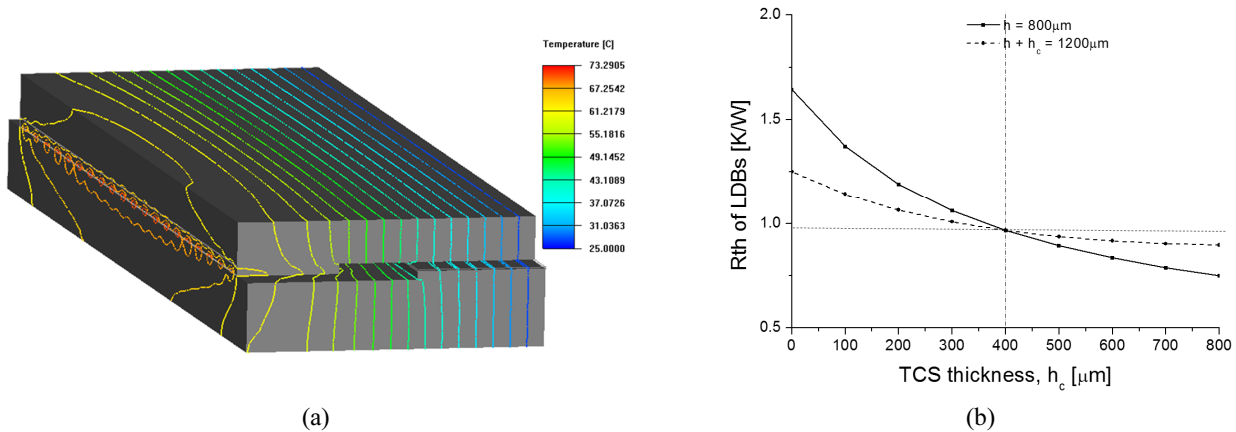


FIG. 4. Thermal-resistance variation of a proposed LDB with a top canopy (TCS) is simulated as a function of top-canopy thickness. (a) Temperature contour map for the top-canopy $h_c = 400 \mu\text{m}$ and submount $h = 800 \mu\text{m}$. (b) The CsR lines of R_{th} for various h_c (fixed $h = 800 \mu\text{m}$, solid line) and h (fixed $h + h_c = 1200 \mu\text{m}$, dotted line) are shown. Note that $h_c = 400 \mu\text{m}$ is the same condition for both lines.

The heat flow looks straight in most regions, except near the active region of the LDB, as seen in Fig. 4(a), and improvement of R_{th} by 50% is possible with minor streamline deformation. Note that $R_{th}=0.94$ K/W for $h + h_c = 1200$ μm is lower than $R_{th}=1.03$ K/W for a typical LDB with $h=2000$ μm , even though the thickness is small. Both CsR curves of $R_{th}(h_c)$ for fixed $h=800$ μm (solid line) and fixed $h + h_c = 1200$ μm (dotted line) in Fig. 4(b) reveal good matching to a simple model analysis with a parallel bypass resistor. The corresponding formula for a parallel- R -network model, shown in Fig. 2, is obtained as given in Eq. (3):

$$R_{th_total} = \frac{1}{\frac{1}{(R_{LD} + R_c)} + \frac{1}{R_H}} \quad (3)$$

It is important to note that the thickness h should be larger than h_c for mechanical support of an LDB, and the total thickness $h + h_c$ should be small, to increase the stacking density. The comparison of three cases, ($h=800$ μm , $h_c=800$ μm), ($h=800$ μm , $h_c=400$ μm), and ($h=800$ μm , $h_c=200$ μm) in Fig. 4(b) helps to understand the process of structural optimization. The improvement of $\sim 19\%$ in $R_{th}=0.76$ K/W for the case ($h=800$ μm , $h_c=800$ μm) from $R_{th}=0.94$ K/W for the case ($h=800$ μm , $h_c=400$ μm) is relatively inefficient, considering the thickness increase of $\sim 33\%$ (1200 to 1600 μm), in comparison to the improvement of $\sim 22\%$ in $R_{th}=0.94$ K/W for ($h=800$ μm , $h_c=400$ μm) from $R_{th}=1.21$ K/W for ($h=800$ μm , $h_c=200$ μm) with a thickness increase of only $\sim 20\%$ (1000 to 1200 μm).

It is now possible to check, in an indirect way, the deterioration of R due to the distortion of the thermal streamline. As the thermal divergence causes thermal streamline distortion, and thus deterioration of R , the thickness variation controls the degree of R -deterioration in R_c and R_h . The change in R -deterioration is easily compared

in the form of the thermal flow ratio, $P_{ratio} = P_c / (P_c + P_s)$, where P_c is the thermal power flow through the canopy and P_s is that through the submount. The thermal flow ratios of TCS as a function of h_c for $h=800$ μm are shown in Fig. 5, with comparison of CsR to SeR (Simply estimated Result) of the divergence-free model. The values of R_c , R_h , and P_{ratio} are also listed in Table 2.

As expected, it is apparent that the estimated contribution of the canopy to the thermal flow is higher in CsR (from simulation) than in SeR (from a simple analytical model), for the entire h_c range in the graph. Moreover, the difference ratio $P_{ratio,CsR}/P_{ratio,SeR}$ becomes smaller as h_c increases, as seen in Fig. 5 for the case of $h=800$ μm , in that while $P_{ratio,CsR} \sim 50$ is just 6% higher than $P_{ratio,SeR} \sim 47$ for $h_c = 400$ μm , $P_{ratio,CsR} \sim 29$ is 20% higher than $P_{ratio,SeR} \sim 24$ for $h_c = 100$ μm . The difference becomes small as it indicates the comparison of R -deterioration between canopy h_c and fixed submount at $h=800$ μm . Note that the $P_{ratio,CsR} \sim 15$ is 50% higher than $P_{ratio,SeR} \sim 10$ even for $h_c = 0$ μm , as it still has a CTE-matched layer of thickness 100 μm .

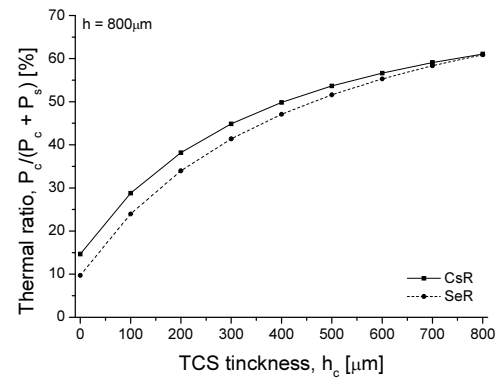


FIG. 5. Variation of thermal-flow ratio as a function of h_c for submount $h=800$ μm . The comparison of the two curves, SeR and CsR, reveals that the difference is larger for thinner canopies.

TABLE 2. Thermal-resistance values from CsR (CFD simulated Result) and SeR (Simply estimated Result), and corresponding R_c , R_h , and $P_{ratio} = P_c / (P_c + P_s)$

Contact sheet thickness [μm]	CsR (CFD simulated Result)			SeR (Simply estimated Result)		
	R_c [K/W]	R_h [K/W]	$P_c / (P_c + P_s)$ [%]	R_c [K/W]	R_h [K/W]	$P_c / (P_c + P_s)$ [%]
0	11.19	1.92	14.68	17.69	1.9	9.69
100	4.76		28.81	6.02		23.97
200	3.11		38.19	3.69		33.98
300	2.37		44.86	2.69		41.39
400	1.94		49.82	2.13		47.09
500	1.66		53.64	1.78		51.61
600	1.47		56.65	1.54		55.29
700	1.33		59.08	1.36		58.34
800	1.23		61.07	1.22		60.91

V. CONCLUSION

As LDBs have found increased application and the need for producing high optical power output increases, issues of cooling and packaging for high-power LDB and stacked LDBs become important. In this paper we proposed an improved heat-sink design for stacked LDBs with a top-canopy structure, and analyzed the efficiency change according to the variation of canopy thickness h_c . The meaning of the P_{ratio} analysis is summarized as follows: First, the use of a top canopy is more efficient than expected from a simple, analytical parallel model. Second, the R-deterioration becomes severe for large thickness, owing to the thermal divergence with streamline distortion. Third, it is better in thermal design to have quasisymmetric thickness in considering the thermal conductivity, as far as the mechanical support permits and the net thermal resistance limit allows.

ACKNOWLEDGMENT

This study was supported by a grant from the special research fund of INHA University.

REFERENCES

1. Y. Izawa, N. Miyanaga, J. Kawanaka, and K. Yamakawa, "High power lasers and their new applications," *J. Opt. Soc. Korea* **12**, 178-185 (2008).
2. B. Liu, X. Tong, C. Jiang, D. R. Brown, and L. Robertson, "Development of stable, narrow spectral line-width, fiber delivered laser source for spin exchange optical pumping," *Appl. Opt.* **54**, 5420-5424 (2010).
3. Y. Y. X. Chen, X. Liu, Y. Mei, G. Q. Lu, "Die bonding of high power 808 nm laser diodes with nanosilver paste," *J. Electron. Packag.* **134**, 041003-1-7 (2012).
4. Y. Qiao, S. Feng, C. Xiong, and H. Zhu, "Working thermal stresses in AlGaAs/GaAs high-power laser diode bars using infrared thermography," *IEEE T. D. M. R* **14**, 413-417 (2014).
5. T. G. Desai, M. Flannery, N. V. Velson, and P. Griffin, "Nanoscale coating for microchannel cooler protection in high powered laser diodes," *Proc. IEEE Modeling & Management Symposium* (San Jose, CA, USA 2015), pp. 336-342.
6. M. Leers and K. Boucke, "Cooling Approaches for High Power Diode Laser Bars," in *Proc. IEEE Electronic Components and Technology Conference* (Lake Blumena Vista, FL, USA, Oct. 2007), pp. 1011-1016.
7. A. Koziwska, P. Lapka, M. Seredynski, M. Teodorczyk, and E. Dabrowsk-Tumanska, "Experimental study and numerical modeling of micro-channel cooler with micro-pipes for high-power diode laser arrays," *Appl. Therm. Eng.* **91**, 279-287 (2015).
8. B. G. Ji, S. G. Lee, S. G. Park, and B. H. O, "Simple thermal diverging model of the thin epitaxial layer of inp laser diodes," *J. Koran. Phys. Soc.* **67**, 1175-1178 (2015).